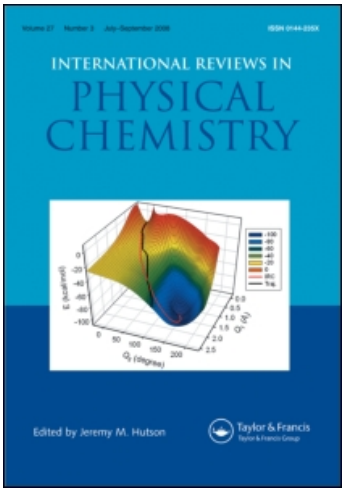

International Reviews in Physical Chemistry
Publication details, including instructions for authors and subscription information:
http://www.informaworld.com/smpp/title~content=t713724383

Picosecond time-resolved photoelectron spectroscopy as a means of gaining insight into mechanisms of intramolecular vibrational energy redistribution in excited states

Katharine L. Reid[a]
[a] School of Chemistry, University of Nottingham, Nottingham, NG7 2RD, United Kingdom

To cite this Article Reid, Katharine L.(2008) 'Picosecond time-resolved photoelectron spectroscopy as a means of gaining insight into mechanisms of intramolecular vibrational energy redistribution in excited states', International Reviews in Physical Chemistry, 27: 4, 607 — 628
To link to this Article: DOI: 10.1080/01442350802229982
URL: http://dx.doi.org/10.1080/01442350802229982

International Reviews in Physical Chemistry
Vol. 27, No. 4, October–December 2008, 607–628

Taylor & Francis
Taylor & Francis Group

Picosecond time-resolved photoelectron spectroscopy as a means of gaining insight into mechanisms of intramolecular vibrational energy redistribution in excited states

Katharine L. Reid*

School of Chemistry, University of Nottingham, Nottingham NG7 2RD, United Kingdom

(*Received 18 March 2008; final version received 22 May 2008*)

We consider the information that can be obtained from time-resolved photoelectron spectroscopy studies of intramolecular vibrational energy redistribution (IVR) in excited states of molecules, focusing on picosecond time-resolved studies of IVR in the intermediate regime. We show that time-resolved measurements may tell us as much about the experimental conditions as they do about the dynamics under examination. We show that carefully controlled picosecond time-resolved photoelectron studies are becoming feasible and that these, combined with robust calculations of Franck–Condon factors, may point the way forward in the quest to understand excited state IVR.

Keywords: intramolecular vibrational energy redistribution; photoelectron imaging; laser photoelectron spectroscopy; excited state dynamics

Contents

*Email: Katharine.Reid@Nottingham.ac.uk

ISSN 0144–235X print/ISSN 1366–591X online

DOI: 10.1080/01442350802229982
http://www.informaworld.com

1. Introduction

Isolated molecules in excited electronic states can undergo a number of competing dynamical processes: predissociation, intramolecular vibrational energy redistribution (IVR), internal conversion and intersystem crossing. These processes in turn compete with fluorescence. An understanding of this whole system of interconnected dynamics is not only of fundamental importance in our understanding of the dynamics of unimolecular reactions, but also underpins the photochemistry of vision, photosynthesis and atmospheric reactions. In this review we concentrate on the application of time-resolved photoelectron spectroscopy to the study of IVR which is the name given to the generic process by which energy relocates from a particular vibrational mode of a molecule into other vibrational modes, with no loss of total energy. There have been a number of recent reviews of the technique of time-resolved photoelectron spectroscopy [1–3] but whereas the others have concentrated on femtosecond time resolution, the focus of the present review is on information that can be obtained when using laser pulses of 1 picosecond in duration. This timescale leads naturally to the study of IVR of small polyatomic molecules in the so-called intermediate regime, in which recurrences of localized vibrational motion can be expected, as opposed to a statistical redistribution of energy.

Although the intramolecular dynamics of molecules in excited states have been a subject of scientific investigation for decades, in most studies the resulting data provide only lifetimes with no insight into the mechanism of energy redistribution. In our work we have shown that even these lifetimes are very dependent on the manner in which the excited state is prepared [4], and carefully controlled studies are therefore badly needed. This situation is in marked contrast to that pertaining to studies of intramolecular dynamics in prepared levels in the electronic ground state of a number of molecules, from which enormous detail has been obtained through frequency-resolved studies enabling the observation of individual eigenstates [5,6]. The difference in the state-of-play for the ground and excited state studies reflects the facts that (i) frequency-domain studies with eigenstate resolution over energy regions of chemical interest in excited states are difficult to perform, and (ii) most time-domain studies lose information concerning the role of individual vibrational motions. As explained later in this review there are advantages and disadvantages of performing eigenstate-resolved and femtosecond time-resolved studies of IVR. Here we make the case for an experiment which represents a compromise between these two extremes. In such an experiment the time and energy resolution of the experimental probe of the dynamics is sufficient to identify the time-dependent vibrational populations on a timescale significantly shorter than the IVR lifetime. This becomes feasible when laser pulses of $\sim$1 ps duration ($\sim$15 cm^{-1} bandwidth) are employed if the

resolution of the IVR probe is determined by the laser bandwidth and not by artefacts of the detection method. However, we also demonstrate the necessity of performing multiple experiments in which the effect of varying aspects of the preparation step are studied, and in which key comparisons are made.

We begin this review with an explanation of the key concepts in IVR and go on to discuss how time-resolved photoelectron spectroscopy can be used as a probe of IVR dynamics. We consider the pros and cons of different methods of photoelectron spectroscopy, and the factors which affect the observations made. Finally, we discuss some recent results concerning IVR in substituted toluenes and point out the questions that still remain.

2. The concept of IVR

Inherent in the concept of IVR is the assumption that molecules can be satisfactorily described as 'balls and springs', and that within this model 'states' can be invoked that evolve in time. The reality must always be that molecular energy levels are accurately represented by the true solutions of the full Schrödinger equation, that the resulting eigenstates are orthogonal and therefore uncoupled, and that time dependence can only result if a superposition of eigenstates is prepared. However, comfort and chemical intuition, not to mention the possibility of computational success, are to be drawn from the Born–Oppenheimer and normal mode separations and their consequences. These consequences include such necessary evils as coupling, perturbations, and the time-dependence of eigenstate superpositions that are nominally considered to be 'states'. Throughout this review the word 'state' will be used to indicate a superposition of eigenstates that results from the assumption that we can use the Born–Oppenheimer separation, and invoke separable vibrational modes.

In this section we consider the situation that results when states are anharmonically coupled to each other. However, the points deduced at the end of the section apply equally well when other kinds of coupling are significant. The essence of IVR is shown in Figure 1 which illustrates the simplest case of a Fermi resonance. Because neither the molecular rotational angular momentum, nor its projection in the molecular frame can change as a result of anharmonic coupling, the inclusion of molecular rotation does not increase the

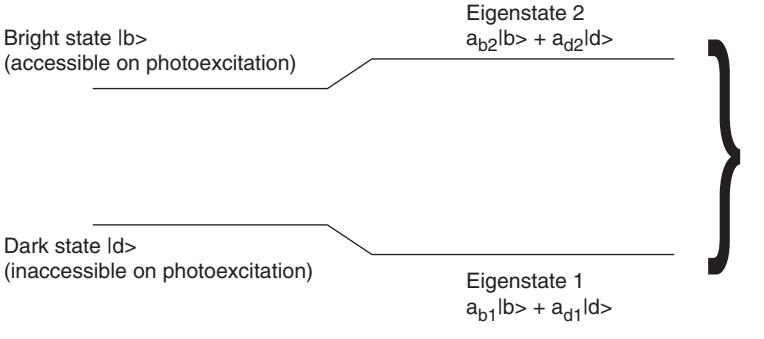

Figure 1. Schematic of the energy level scheme pertaining to a Fermi resonance; the simplest situation that gives rise to IVR.

number of coupled levels in Figure 1 which can be considered to be the picture resulting for any given defined rotational state. The bright and dark states in the Figure are harmonic vibrational levels in an excited electronic state, each associated with a specified normal mode. An optical transition to the bright state from the ground electronic state is allowed by symmetry and has a significant Franck–Condon factor. An optical transition to the dark state is either symmetry forbidden or has a negligible Franck–Condon factor.

The bright and the dark state are coupled to each other by anharmonicity to give two eigenstates both of which therefore have some bright and some dark state character. In an eigenstate-resolved experiment, each of the two eigenstates can be separately prepared and no time evolution can occur. In order for time evolution to occur the excitation bandwidth must be sufficient to encompass the two eigenstates; the short laser pulses used in time-resolved studies mean that the preparation of such superpositions is the norm. In this instance, the superposition of eigenstates at time zero resembles the bright state, and a dark state signature appears as time goes on. In the simple two-level example given in Figure 1 an oscillation of intensity could be observed with a period that is inversely dependent on the eigenstate energy separation if a suitable experiment were performed (see later).

The typical IVR scenario would involve the generalization of Figure 1 to an n-level situation with one bright state and $n-1$ dark states which are coupled to the bright state by anharmonicity. If the bright state and dark states give rise to only a few eigenstates that are simultaneously prepared then recurrences can be observed. If, however, the bright state is composed of many eigenstates then the statistical regime is accessed and energy flows irreversibly away from the bright state. The energy redistribution 'mechanism' is determined by the coupling matrix elements between the bright state and the various dark states, and the magnitudes of these coupling matrix elements provide chemical insight via the deduction of the routes through which energy can flow. Therefore, studies of mechanisms of intramolecular energy redistribution seek to identify the dark states and determine the coupling matrix elements. Even better is the observation of the time-dependent population of all possible dark states as this gives insight into the 'critical' couplings that facilitate the loss of energy from the bright state via so-called 'doorway states'.

Some important lessons that are equally applicable to the many level case can be learned from examination of Figure 1.

(i) Time dependence can only be observed if the bandwidth of the light in the excitation process is sufficient to encompass more than one molecular eigenstate. In other words, an absence of time dependence does not necessarily mean that there is no IVR.

(ii) If more than one bright state is encompassed by the bandwidth then time dependence can result that is unrelated to IVR (this is analogous to the preparation of a vibrational wavepacket in a diatomic molecule – see below).[1] The measurement of an absorption spectrum with a bandwidth narrow enough to selectively excite individual bright states is needed to guard against this.

(iii) The time dependence observed will only reflect the full IVR process if the bandwidth is sufficient to encompass *all of* the eigenstates arising from the bright state and any dark states to which it is coupled.

(iv) If the excitation bandwidth is sufficiently narrow to resolve individual eigenstates (this would necessitate resolving rotational levels) then no time dependence can be observed, but IVR can be inferred from the eigenstate energies and intensities in the absorption spectrum.

It will be clear from the above that experiments that are intended to probe IVR processes need to be carefully conceived and the results carefully interpreted. Undoubtedly, eigenstate-resolved experiments are the 'safest' to interpret. However, these experiments are hugely difficult to perform on excited states, and the mass of resulting lines in the spectrum do not naturally map onto a simple chemical picture. Thus, most studies have concentrated on the situation when single eigenstates cannot be resolved, with the exception of the pioneering work of Pratt and coworkers [7].

Generally, experiments that have been used to study IVR in excited states fall into two camps: dispersed fluorescence [8,9] and photoelectron spectroscopy [10–12], either of which can be performed in a time-resolved or non-time-resolved fashion. In these experiments the IVR process will cause different vibrational levels in the ground state (dispersed fluorescence) or ion (photoelectron spectroscopy) to be populated, and thus a Franck–Condon fingerprint of the contributing dark states can be observed which is time-dependent. This time dependence can be used to extract an IVR lifetime or rate [13], and in principle the dark states populated as a function of time can be identified from their Franck–Condon fingerprint. In such experiments scientists must take great care to understand exactly what they have prepared, what their measurements imply, and how they can be realistically compared with other measurements.

3. Prototype experiment

Over the last few years, the use of time-resolved photoelectron spectroscopy as a probe of excited state dynamics has been gaining momentum worldwide [1,2,3,14]. The technique is powerful in that (i) the kinetic energies of the photoelectrons provide information on the internal states of the ion formed, which in turn reflect the levels populated in the excited state, (ii) ionization is a universal detection method for excited state species, and (iii) such a 'pump–probe' technique gives a well-determined and controllable time-delay between the preparation of the initially prepared 'bright state' (by the pump pulse) and the moment of interrogation (by the probe pulse).

An opportunity to illustrate the prototype time-resolved photoelectron spectroscopy experiment, that also provides a simple illustration of the fact that the observation of time evolution of an initially prepared state does not necessarily imply IVR, is given by the preparation of a vibrational wavepacket in an excited electronic state of a diatomic molecule [15,16]. In this instance there are no selection rules controlling the vibrational states that can be prepared, i.e., all the states lying within the bandwidth are bright. In a typical experiment a superposition of excited state vibrational eigenstates ϕ_n, each with energy E_n, would be prepared with a femtosecond laser pulse. This causes the expectation value of the displacement $\langle x \rangle$ of the bond length in the excited state from its equilibrium value to oscillate according to:

$$\langle x \rangle = \sum_{n,m} a_n^* a_m e^{(i(E_n - E_m)t)/\hbar} \langle \phi_n | x | \phi_m \rangle. \tag{1}$$

This time evolution is caused by an evolving phase relationship between the eigenstates forming the initially excited superposition, with the contribution of each eigenstate weighted by the relevant Franck–Condon factor and the light intensity at the frequency required to prepare it; these two factors give rise to the values of the coefficients a_n in Equation (1). According to Equation (1) oscillations will occur indefinitely; in practice of course they will gradually decay as the excited state radiates. In order to observe this oscillation a second femtosecond laser pulse can be used to ionize the molecule after a defined time delay; this is illustrated in Figure 2. If a fortuitous relationship between the potential energy curves of the excited state and the ion exists, as in Figure 2, a time evolution can be observed in the intensity of ions or photoelectrons produced. Just as the Fermi resonance discussed above provides a prototype for the IVR process, the diatomic wavepacket provides a prototype for an experiment that can be used to probe IVR and gives us further insight into the origins of time evolution.

In IVR processes time evolution can also be explained by an evolving phase relationship between eigenstates, but because those eigenstates can be considered to result from couplings between states the phase evolution promotes the redistribution of energy around the molecular framework, sometimes irreversibly. In addition, whereas in the diatomic vibrational wavepacket case a set of bright states is prepared within the excitation bandwidth, in time-resolved IVR studies ideally only a single bright state is prepared, with other harmonic vibrational levels lying within the bandwidth being inaccessible to optical excitation. In this instance, if one can be certain that only a single bright state was prepared, then the observation of any time evolution must be a consequence of IVR.

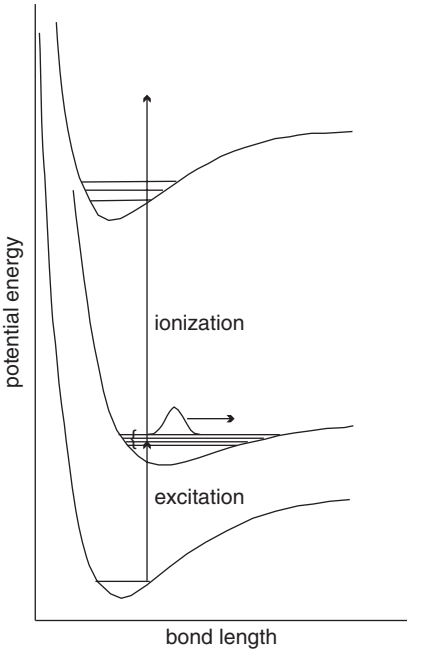

Figure 2. Schematic of an experiment that can be used to probe a vibrational wavepacket that has been formed in an excited state of a diatomic molecule.

Rotational selection rules dictate that a single bright state will in fact be composed of more than one rotational state in the form of a rotational wavepacket. However, because the evolution of this wavepacket will not affect the Franck–Condon factors connecting the bright state to vibrational levels in another electronic state this will cause neither photoelectron spectra nor dispersed fluorescence spectra to evolve in time. Evidence of the existence of the rotational wavepacket can however be found by using other measurements as explained in Section 5.

4. Photoelectron methods

Much of the activity in time-resolved photoelectron spectroscopy has been precipitated by developments in femtosecond laser technology, as well as in photoelectron imaging methods. The reasons for the success of imaging techniques are the ease of measurements, the excellent collection efficiency, and the fact that photoelectron angular distributions are simultaneously acquired at no extra cost. Femtosecond time-resolved experiments have an energy resolution that is limited by the bandwidth of the laser pulses (typically $\sim 100\,\mathrm{cm}^{-1}$) which rarely allows for the resolution of individual vibrational levels and is well matched by the resolution typically achieved in photoelectron imaging. However, in the experiment we considered at the start of this article laser pulses would be sufficiently short to monitor dynamics in real time, and yet have sufficiently narrow bandwidth ($\sim 15\,\mathrm{cm}^{-1}$) to enable vibrational resolution of the ion formed. In order to take advantage of the narrow bandwidth it is necessary to employ a method of photoelectron detection with resolution approaching the bandwidth. In what follows we focus on the information that can be obtained from different methods of photoelectron spectroscopy when applied to time-resolved studies. The reader is referred elsewhere for details of the techniques [1].

4.1. *ZEKE*

The photoelectron method with the ultimate resolution is ZEKE, as originally developed by Müller-Dethlefs and coworkers [17]. In ZEKE spectroscopy of excited states a pump laser is used to prepare an initial level, and a probe laser is tuned to be resonant with an ionic internal energy level. Those electrons formed at threshold (or actually those electrons that result from the field-ionization of high lying Rydberg states [18]) are then extracted by an electric field and detected as a function of the probe laser frequency. The resolution of the technique is limited only by the laser bandwidth, however its disadvantages are that (a) the experiments are extremely time-consuming compared with other methods of photoelectron spectroscopy, (b) it is necessary to have a probe laser that can be scanned over the region of interest, preferably with no change in intensity, and (c) only those electrons formed at threshold can be used as a probe. The first two disadvantages limit the range of cation energies that can realistically be studied, and are even more severe in time-resolved studies. As a consequence, very little work has been done which employs time-resolved ZEKE. Some pioneering work using this method to study IVR was undertaken by Knee and coworkers who used laser pulses of ~10–15 ps duration to study IVR in *p*-difluorobenzene [19] and fluorene [20], and in the anline-CH_4 van der Waals complex [21]. In Figure 3 we show a ZEKE spectrum measured by Knee and coworkers following excitation of a vibrational level in fluorene that is at $834\,\mathrm{cm}^{-1}$ above the S_1

origin with a 10 ps laser pulse with a bandwidth of $6\,cm^{-1}$, and ionization with a 10 ps laser pulse that is overlapped in time. The resolution obtained is limited only by the laser bandwidth, enabling vibrational structure to be clearly seen. In this experiment time-resolved measurements were made by fixing the probe laser to a single wavelength corresponding to a peak in Figure 3 and monitoring the ZEKE signal as a function of time delay; it was not possible to measure ZEKE spectra over significant cation energies at each time delay. Despite the fact that the field has been left relatively unexplored since the initial work, ZEKE is an important technique to have available because its exceptional resolution can enable it to reveal information that is hidden to other methods. In the future its main power in this area is likely lie in its use as a complementary technique to velocity map imaging (see next section) where it can provide a high-resolution picture of a narrow range of cation energies that have been previously been revealed to be of dynamical interest.

4.2. *Velocity map imaging*

Velocity-map imaging (VMI) of photoelectrons has gained enormous impetus since its first demonstration by Eppink and Parker [22]. Although more sophisticated methods that enable the position sensitive detection of photoelectrons have since been, and continue to be, developed with the aim of improving the information available on the full three-dimensional photoelectron distribution [23,24], VMI continues to be popular because of its ease of use and its excellent collection efficiency. The resolution of VMI depends on the number of pores in the microchannel plate detector, the resolution of the camera used to record the image, the size of the image, and the total energy, E, available to the photoelectrons. The state-of-the-art resolution is quoted in the literature as $\Delta E/E = 0.38\%$ [25], and thus with a photoelectron kinetic energy of $2000\,cm^{-1}$ it would be in principle possible to resolve features lying further than $\sim 10\,cm^{-1}$ apart if the laser bandwidth were less than this. However, most experiments are far from this state-of-the-art, with $\Delta E/E = 5\%$ being more common in practice. In a typical VMI experiment in which an excited state is prepared and ionized the pump and probe wavelengths will be the same, constraining E and therefore limiting the achievable energy resolution (but see Section 4.3). In femtosecond time-resolved experiments this does not

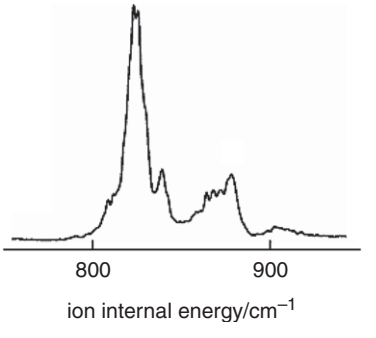

Figure 3. Picosecond ZEKE spectrum of fluorene, see text. Reused with permission from J. M. Smith, J. Chem. Phys., **93**, 4475 (1990). Copyright 1990, American Institute of Physics, Ref. [20].

present much of a disadvantage because the laser bandwidth will often be the absolute limit on resolution. The use of VMI in femtosecond time-resolved photoelectron spectroscopy was pioneered by Suzuki and coworkers [26], and the first example is shown in Figure 4. In this study Suzuki and coworkers used laser pulses of ~400 fs duration to prepare pyrazine in its S_1 electronic state and observed the dynamics of intersystem crossing [26]. For the purposes of following intersystem crossing processes the resolution afforded by the VMI technique is clearly appropriate. In this instance it can be seen that the full width at half maximum of the narrowest peak in the spectrum is around 50 meV, or 400 cm^{-1} and the resolution is limited by the detection method. Femtosecond time-resolved VMI has been successfully applied to the study of energy redistribution processes in neutral molecules [12,26,27], and in anions [28,29], and in some of these studies photoelectron angular distributions have also been analysed, see Section 5. However, we note that the photoelectron spectra obtained have insufficiently good resolution to enable the characterization of dark vibrational states that may have been populated by IVR; such resolution is generally precluded by the laser bandwidth.

4.3. *SEVI*

Neumark and coworkers [30] have adapted a method known as 'slow electron velocity imaging', which was pioneered by Vrakking and coworkers [31], to high-resolution photoelectron spectroscopy over an extended energy range. This technique is a compromise between VMI and ZEKE, borrowing advantages and disadvantages from each, and relies on reducing the total available energy E to make $\Delta E/E$ as small as possible. In its simplest form, SEVI is a two-colour version of VMI, i.e. the wavelengths of the pump and probe laser beams are different from each other. This enables the probe wavelength to be chosen to generate slow electrons associated with an ion internal energy state of interest. The image of these electrons is then expanded to fill the detector by the choice of appropriate voltages, so that the number of pixels separating each photoelectron peak is maximized. Unlike in ZEKE the probe wavelength is not scanned, but in the

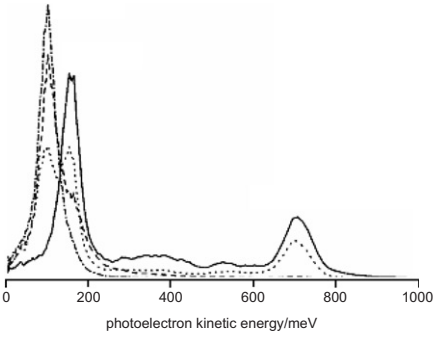

Figure 4. Femtosecond photoelectron VMI spectrum at four different time delays: Solid line 0.3 ps, dotted line 30 ps, dashed line 200 ps, dash-dot 500 ps. The two main peaks on the left-hand side correspond to triplet states of the neutral whereas the peak on the right-hand side corresponds to the prepared S_1 state. Reused with permission from T. Suzuki, J. Chem. Phys., **111**, 4859 (1999). Copyright 1999, American Institute of Physics, Ref. [26].

adaptation of SEVI by Neumark and coworkers it is stepped in order to focus on each ion internal energy state, and the resulting spectra corresponding to each probe wavelength are combined to give the full spectrum. Thus, the experiments fall between VMI and ZEKE in terms of the length of time they take to perform and the resolution obtained, while still retaining good collection efficiency and angular information. They also have the advantages that (i) in situations where the molecule can be ionized with two photons at the pump wavelength a 'one-colour' VMI experiment can be performed initially with no changes to the apparatus, and (ii) the excess energy can be chosen, unlike in ZEKE where only threshold electrons are detected. In Figure 5 we show an example of the improvement in resolution that can be obtained by using the SEVI technique for just a single probe wavelength [32]. The photoelectrons produced have a maximum of 5240 cm^{-1} kinetic energy in the VMI spectrum and 2240 cm^{-1} in the SEVI spectrum, and the peak widths in the spectrum reduce accordingly by at least a factor of 3. As we show in Section 7.4 the SEVI technique is beautifully matched to the needs of our 'ideal' experiment.

5. PADs

In the velocity map imaging method, or its SEVI variant, the measurement of a photoelectron angular distribution (PAD) [33] occurs automatically. Time-resolved photoelectron angular distributions have been shown to be powerful probes of the dynamics of photodissociation [23, 34], intersystem crossing [26,35] and internal conversion [36], and have also been used to monitor the evolution of a pure rotational wavepacket [37,38], in a version of rotational coherence spectroscopy [39]. In general, time-resolved PADs are expected to yield useful information when either a molecule is undergoing a transition between states of different symmetry, or when changes in molecular alignment provide a probe of a dynamical process [40]. In the case of IVR, the time evolution of molecular alignment can, in principle, be used to diagnose the

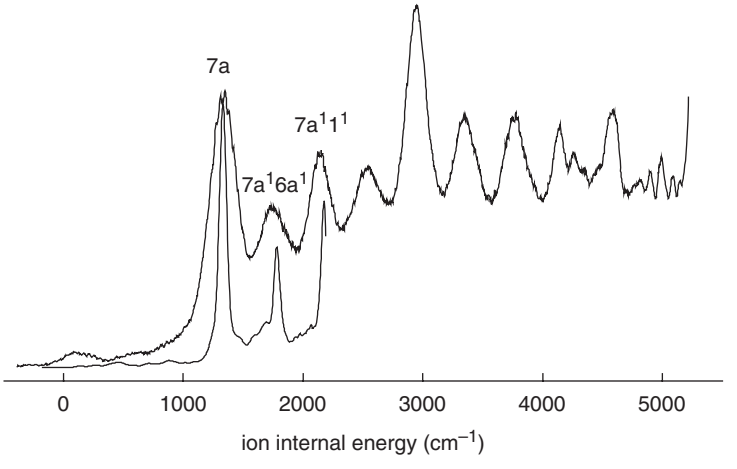

Figure 5. Comparison of the VMI (upper trace) and SEVI (lower trace) methods of photoelectron spectroscopy. The spectra are taken using 1 ps laser pulses to excite *p*-fluorotoluene to its $7a^1$ level in S_1 and 1 ps laser pulses to ionize (see text).

involvement of Coriolis coupling in the redistribution process [41–44]. This is expected because the conservation of total angular momentum leads to a change in its molecular frame projection when the Coriolis interaction of vibration and rotation occurs. This in turn means that although the laboratory frame projection of the total angular momentum (and therefore the angular momentum alignment in space) remains fixed, the molecular axis alignment changes as a consequence of the Coriolis interaction. Therefore any observable that is sensitive to molecular axis alignment, such as fluorescence polarization [42] or PADs [42–44] should in turn be sensitive to Coriolis coupling. However, it has been observed that in the aromatic molecules most favoured for studies of excited state IVR PADs are typically close to isotropic and show little if any dependence on pump–probe time delay [12,45]. The reasons for this are likely to be a combination of the relatively small alignment it is possible to create following a one-photon π–π^* transition involving a benzene ring, and the relative insensitivity of the photoelectron wavefunction to molecular alignment when the electron is ejected from an aromatic π^* orbital. However, in a pioneering fluorescence polarization study Nathanson and McClelland demonstrated a sensitivity to Coriolis coupling when only a small alignment was prepared on excitation [46], and so it seems likely that it is the ionization dynamics that limit the sensitivity of PADs to alignment. In a further complication, there is now evidence that a number of small aromatic molecules show shape resonance behaviour near threshold which causes the PADs to depend strongly on the electron kinetic energy [45,47]. The handful of molecular systems in which a strong alignment sensitivity has been observed all involve the ejection of electrons from non-bonding, localized bonding, or Rydberg orbitals, or from anions. However, with developments in laser technology the study of an increasing number of molecular systems is becoming tractable, and in the future it is likely that time-resolved PADs will be shown to hold useful dynamical information for some systems.

6. Factors influencing the observations made in time-resolved photoelectron spectroscopy studies of IVR

6.1. *Preparation method*

In Figure 6 we illustrate a scenario in which strongly and weakly coupled levels contribute to an IVR process. In this scenario a narrow excitation bandwidth would cause no time-evolution, but would be sensitive to the coupling of two harmonic oscillator levels. A broader excitation bandwidth would enable the preparation of a time-varying superposition, but the time variation would only reflect weak coupling. Only if the excitation bandwidth were sufficiently broad to prepare the two levels resulting from the strong coupling of n and m would any observed time behaviour reflect the true IVR situation. Thus, the excitation bandwidth is crucial and will affect the experimental observables. We also note that the frequency *profile* of the excitation laser beam will have a bearing on what can be observed as it will determine the (time-independent) population of each molecular eigenstate. It is also worth mentioning that at high photon density, as well as the possible effects of saturation, power broadening and the absorption of multiple photons, it is possible that the rate of ionization will exceed the rate of energy redistribution in the molecule, even if the laser pulses are longer than the redistribution lifetime. Therefore the time resolution of the experiment is not necessarily determined by the laser pulse duration.

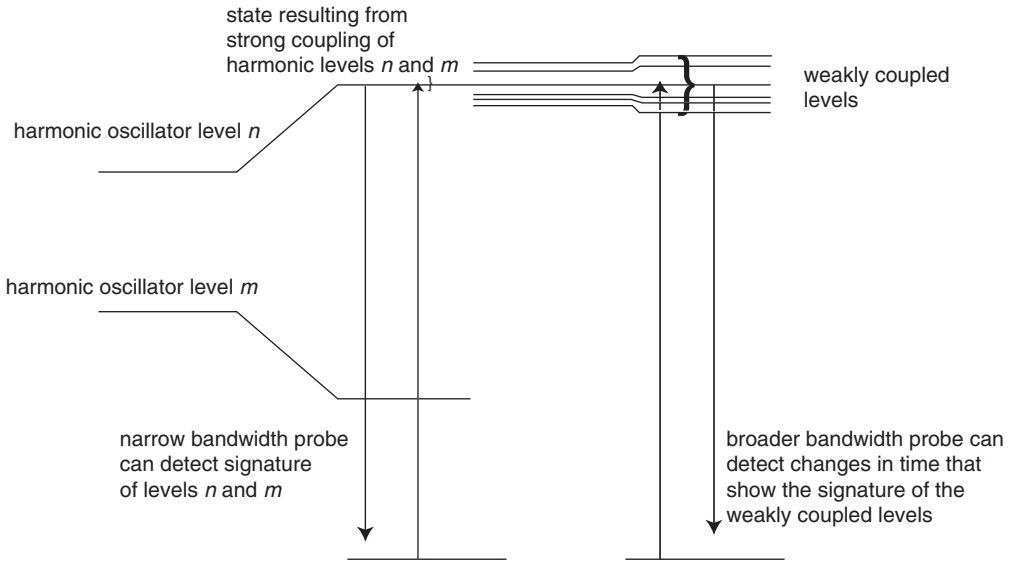

Figure 6. Schematic to illustrate that strongly coupled levels may not give rise to time dependence.

6.2. *Detection method*

It is clear from Section 4 that different methods of photoelectron spectroscopy have very different resolution. This in turn affects the dynamics that can be revealed in a given experiment. In an experiment in which the ultimate resolution is not limited by the laser bandwidth it is worth comparing the photoelectron spectra that would result from different techniques, as shown for example in Figure 5 above. As well as features in spectra being masked by poor resolution, artefacts can also result. In Figure 7 we show an example of a comparison between ZEKE and VMI photoelectron spectra of the same two S_1 bands in *p*-fluorotoluene, in this case in a nanosecond experiment. In such an experiment congestion is used as a diagnostic of IVR. However, from Figure 7 it can be seen that whereas the VMI spectrum suggests a congested photoelectron spectrum for both bands, the ZEKE spectrum only shows congestion for one of the two. This constitutes another 'health warning' for the field of time-resolved photoelectron spectroscopy.

7. IVR in substituted toluenes

In this section we draw together the results of some of our studies, and those of other groups, on our test case molecule, *p*-fluorotoluene (*p*FT) and some of its cousins, and relate what we have found to the points made above. Our interest in *p*-fluorotoluene (*p*FT) and toluene was originally inspired by the work of Parmenter and coworkers whose studies implicated the torsional motion of the methyl rotor in *p*FT as an accelerator of IVR in this molecule, relative to *p*-difluorobenzene (*p*DFB) [48–50]. In principle, the hindered rotation of the methyl group in *p*FT and other such molecules can complicate the simple picture of IVR shown in Figure 1 because of the interaction between the methyl group and the benzene ring. However, the torsional barriers in such molecules are generally low

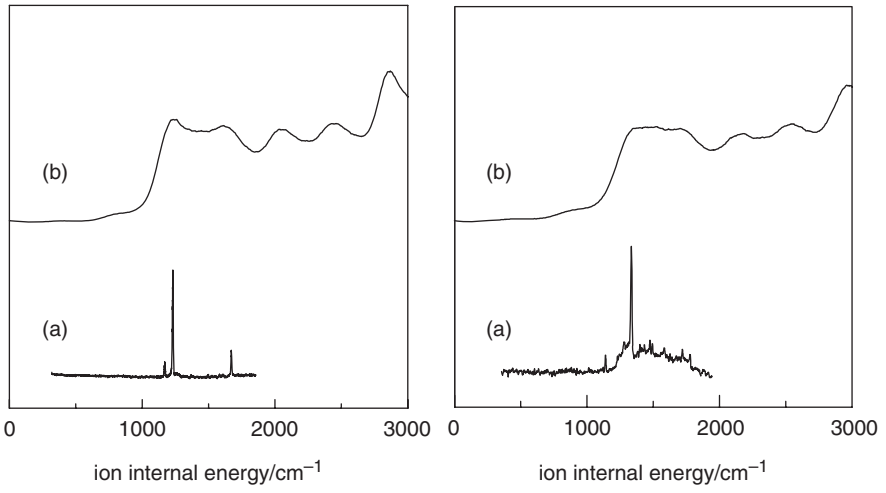

Figure 7. Comparison of (a) ZEKE with (b) VMI following the preparation of two levels in S_1 *p*-fluorotoluene; 13^1 (left panel) and $7a^1$ (right panel) with a 5 ns laser pulse. Reused with permission from C. J. Hammond, J. Chem. Phys., **125**, 124308 (2006). Copyright 2006, American Institute of Physics, Ref. [4].

Table 1. Torsional barrier heights of some substituted toluenes. V_6 is the barrier to 6-fold rotation, and V_3 is the barrier to 3-fold rotation.

Molecule	Torsional barrier height	Reference
Toluene	$\lvert V_6\rvert = 26.4\,\text{cm}^{-1}$	[7]
o-Fluorotoluene	$\lvert V_3\rvert = 21.8\,\text{cm}^{-1}$ $\lvert V_6\rvert = 13.8\,\text{cm}^{-1}$	[60]
m-Fluorotoluene	$\lvert V_3\rvert = 123.7\,\text{cm}^{-1}$ $\lvert V_6\rvert = 26.4\,\text{cm}^{-1}$	[60]
p-Fluorotoluene	$\lvert V_6\rvert = 33.7\,\text{cm}^{-1}$	[60]
D_3 *p*-fluorotoluene	$\lvert V_6\rvert = 25.2\,\text{cm}^{-1}$	[52]

(see Table 1), and for energies above the barrier the methyl group acts as a free rotor with no interaction with the benzene ring. A simple expectation therefore is that there should be a relationship between the torsional barrier height and the rate of IVR following the deposition of energy into modes affected by the torsional motion. Such a relationship was indeed established by Perry and coworkers for a set of small molecules [51], but they found that IVR was faster following the deposition of energy into a vibrational mode near to the centre of flexibility when the torsional barrier was *low*. On the other hand, Borst and Pratt [7] found that in the case of S_1 toluene such a relationship was inconsistent with details of the rotational structure and proposed that a hyperconjugative effect caused an acceleration of IVR in this system. Neither of these studies explicitly considered any mode dependence of the IVR rate. From the previous sections of this review it will also be clear that great care has to be taken to fully understand the influence of the experimental conditions on the observations that are made to ensure that comparisons are valid.

Table 2. IVR lifetimes deduced from experiment following the preparation of the $7a^1$ CF stretching mode in S_1 *p*-fluorotoluene.

Temperature	Excitation bandwidth	Detection method	Deduced IVR lifetime	Reference
300 K	$2\,cm^{-1}$	Dispersed fluorescence/chemical timing	15 ps	[50]
20 K	$5\,cm^{-1}$	Gated dispersed fluorescence	∞	[9]
20 K	$20\,cm^{-1}$	Time-resolved photoelectron spectroscopy/VMI	26 ps	[12]
20 K	$20\,cm^{-1}$	Time-resolved photoelectron spectroscopy/SEVI	19 ps	[32]

7.1. *Experimental variables*

There have been several studies of IVR following the preparation of the $7a^1$ level in S_1 *p*FT, where 7a is a CF stretching mode at $\sim$1200 cm^{-1}, and this provides a useful benchmark for comparison. The results of these experiments are summarized in Table 2. In the experiments of Parmenter and coworkers dispersed emission was monitored following the technique of 'chemical timing' in which a quencher gas at varying pressures is used to limit the excited state lifetime of molecules in a bulb at 300 K, enabling them to make a crude determination of an IVR lifetime of 15 ps [50]. Zewail and coworkers [9] studied time-resolved dispersed fluorescence decays of a jet-cooled sample of *p*FT and found no discernible redistribution following the preparation of levels up to 1600 cm^{-1} using laser pulses of 5 cm^{-1} bandwidth and a detection time resolution of 300 ps. Zewail and coworkers attributed the discrepancy between their work and that of Parmenter and coworkers to the difference in temperature of the sample. In our own work we used a jet-cooled sample and deduced an IVR lifetime of 26 ps from picosecond time-resolved photoelectron spectra [12,32], using the kinetic formalism developed by Parmenter [13]. It will be clear from Table 2 that the lifetimes deduced by Parmenter's group and our group are in reasonable agreement, but that they are in severe disagreement with the observations of Zewail and coworkers. It is difficult to attribute this disagreement to one cause because there are several variables which have been changed, see Table 2.

7.2. *Structural modifications*

In pursuing details of the IVR mechanism, systematic modification of the molecular structure is expected to give valuable information when the same vibrational state is prepared. Preliminary work in this direction was undertaken by Moss and Parmenter who compared the IVR lifetimes following the preparation of the S_1 $7a^1$ level in *p*FT with that in D_3-*p*FT [52], and also with that in *m*-fluorotoluene (*m*FT) [53]. It was found that deuteration decreased the IVR lifetime only by about a factor of 2 relative to *p*FT when comparable energies were studied, an increase rather less than would be predicted from the increased density of states that results from the presence of the heavier atoms. However, the IVR lifetime was decreased by a factor of twelve when the fluorine was in the *meta* compared with the *para* position. They rationalized this by postulating an increased coupling between vibration and internal rotation for the *meta* structure which is consistent with the fact that the torsional barrier in S_1 *m*FT is four times larger than that in S_1 *p*FT.

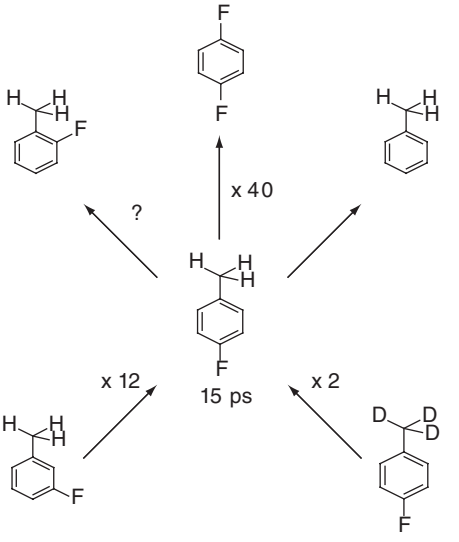

Figure 8. A comparison of IVR lifetimes determined from experiment following the preparation of the $7a^1$ CF stretching mode in S_1. This mode does not exist in toluene, but it is interesting to ask how it fits into the picture.

Although this is inconsistent with the relationship established by Perry and coworkers [51] the motion associated with the CF stretching mode could be argued to be far from the centre of flexibility. The results of these studies are summarized in Figure 8. Clearly such comparative studies are of great importance, however an additional significant question concerns the effect of exciting different vibrational modes on the picture given in Figure 8. Some progress along these lines is given in Sections 7.4 and 7.5.

7.3. *Fermi resonance in S_1 toluene*

A simple illustration of both the power and the drawbacks of picosecond time-resolved VMI photoelectron spectroscopy, and a useful 'proof of principle', is given by a recent study in which we coherently prepared the two eigenstates resulting from a Fermi resonance at $\sim$460 cm^{-1} in S_1 toluene with a 1 ps laser pulse [54]. This Fermi resonance comprises the harmonic oscillator levels $6a^1$ and $10b^116b^1$, giving eigenstate energies at 457 and 462 cm^{-1} [55]. Mode 6a corresponds to a totally symmetric ring-breathing motion, 10b to a B_1 symmetry CH_3 wagging motion, and 16b to a B_1 CH out-of-plane motion, assuming C_{2v} symmetry. In Figure 9 we show the behaviour of the photoelectron spectrum as a function of the delay between the preparation of the wavepacket and its subsequent ionization with a second 1 ps laser pulse of the same wavelength.

In Figure 9 clear oscillations are observable in the photoelectron spectrum as a function of time, and, critically, the sensitivity of the photoelectron signal to the S_1 wavepacket evolution can be seen to depend on the ion state formed. The span of ion internal energies and time delays is far greater than would typically be obtained in a time-resolved ZEKE experiment, in which an extensive wavelength scan would be needed

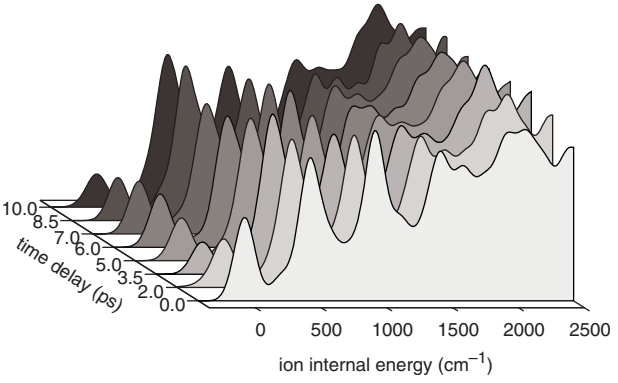

Figure 9. Photoelectron spectra following the preparation of the toluene S_1 Fermi resonance at 457 cm^{-1} with a 1 ps laser pulse, as a function of the time delay between excitation and ionization with a second identical laser pulse. Reused with permission from C. J. Hammond, Journal of Chemical Physics, **124**, 201102 (2006). Copyright 2006, American Institute of Physics, Ref. [54].

for each time delay. Although the vibrational levels in the ion are not fully resolved, clear vibrational structure can be discerned enabling such a measurement to 'point the way' for a subsequent higher resolution experiment in which critical time delays and cation energies could be investigated in greater detail. If ZEKE were used this would enable the resolution of all ion vibrational levels, including torsional levels of the methyl rotor which may be critical to the understanding of the dynamics of molecules such as toluene; most of this structure could also be resolved using the SEVI technique at significantly less experimental cost. This study indicates that the sensitivity to the evolution of a prepared excited state level will depend on the levels accessed in the probe step. In this instance neither the total photoelectron intensity nor the photoelectron spectrum corresponding to ion states with more than ~1500 cm^{-1} internal energy showed any sensitivity to changes in the excited state. This reflects the fact that some vibrational coordinates will be relatively unaffected by IVR involving orthogonal vibrational modes.

7.4. *IVR in p-fluorotoluene*

In recent work [4,12,56] we have sought to study the influence of the nature of the vibrational mode prepared by comparing the IVR lifetimes following selective excitation of the $7a^1$ and 13^1 levels in *p*-fluorotoluene which are separated by only 36 cm^{-1}, and correspond to the excitation of a CF stretching mode and a C–CH_3 stretching mode, respectively. In these time-resolved studies we have used 1 ps laser pulses to excite and ionize. We originally used field-free time-of-flight photoelectron spectroscopy [56] which we subsequently replaced with VMI [12], and more recently we have studied the $7a^1$ level in more detail using SEVI [32], although with only a single probe wavelength to date. We have also made use of nanosecond experiments and so are also able to compare time-averaged with time-resolved studies; in one such study we employed ZEKE [4]. An apparent contradiction occurs in the nanosecond and picosecond results concerning the mode dependence. In the picosecond work of King *et al*. [12] the IVR can be seen

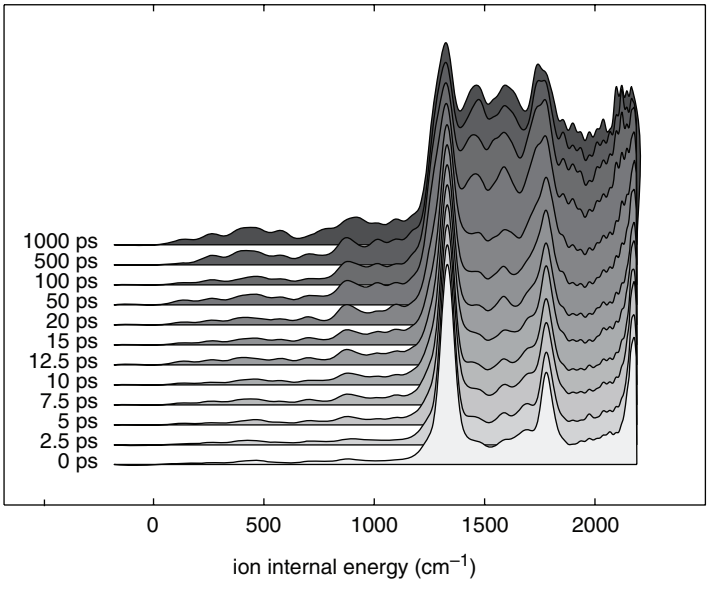

Figure 10. Picosecond time-resolved photoelectron spectra following the preparation of the $7a^1$ level in S_1 *p*-fluorotoluene. The ionization wavelength is to the red of the excitation wavelength [32].

qualitatively to be significantly faster following the excitation of 13^1 compared with $7a^1$, with provisional lifetimes of 16 ps [57] and 26 ps [12], being deduced, respectively. However, the nanosecond ZEKE photoelectron spectra shown in Figure 7 clearly show more structure at long time for the 13^1 excitation, suggesting a longer IVR lifetime for this level [4]. The advent of IVR following the excitation of $7a^1$ can be seen in the appearance of the 'hump' resulting from the ionization of dark states in the ZEKE spectrum in the right panel of Figure 7, whereas the ZEKE spectrum following the excitation of 13^1 case is highly structured. This has so far been rationalized as being a consequence of the much narrower bandwidth ($\sim$0.3 cm^{-1}) in the nanosecond experiments, compared with the picosecond experiments ($\sim$15 cm^{-1}). However, clearly more studies are needed to investigate this further.

In recent work we have adopted the SEVI technique in our picosecond time-resolved experiments, with considerable success. We have already shown in Figure 4 the improvement in resolution that can be obtained over VMI by comparing photoelectron spectra following the preparation of *p*-fluorotoluene in the $7a^1$ level (1230 cm^{-1}) of its S_1 state with the 1 ps pump and probe laser beams overlapped in time. In Figure 10 we show the consequences of this improved resolution for the characterization of dark states. In this Figure SEVI spectra are shown as a function of time delay between pump and probe following the excitation of $7a^1$ in *p*FT. It can be seen that significant changes in the spectra occur in between the major peaks in each spectrum; these features would not have been observable in the VMI spectrum.

The relatively simple structure of the zero-time spectrum is quickly convoluted by the appearance of new spectral features resulting from the ionization of dark states populated with increasing time. Of the three unresolved peaks in between the first two intense peaks

(assigned to the ion vibrational states $7a^1$ and $7a^16a^1$) the intensities of the first two at $1400\,cm^{-1}$ and $1600\,cm^{-1}$ steadily increase with increasing time delay, while the intensity of the third at $1700\,cm^{-1}$ increases initially but begins to fall at around 15 ps. There are also two groups of features at lower ion internal energies than the $7a^1$ peak which are initially weak but gain in intensity with increasing time delay. By 15 ps, the relative intensities of the peaks at lower ion internal energy than $7a^1$ have increased substantially. It is instructive to compare the spectra with the measured nanosecond ZEKE spectra. Although these peaks are not present in the $7a^1$ ZEKE spectrum, peaks at these energies do appear in the $6a^2$ ZEKE spectrum [4]. The S_1 $6a^2$ level cannot be prepared under the bandwidth of the excitation pulse, but the higher overtone $6a^3$ falls neatly within the appropriate range [58]. Moreover, $6a^3$ vibrational state has A_1 symmetry and is dark as a result of a low Franck–Condon factor, and in general ν_{6a} has been found to be highly active [56]. A further connection can be drawn from the presence of the $7a^1$ peak in the $6a^2$ ZEKE spectrum [58]. If $7a^1$ and $6a^3$ were coupled in S_1 then as time goes on we would expect to see transitions to $6a^1$ and $6a^2$ in the ion. These peaks can indeed be seen in the photoelectron spectra at later time delays. We would also expect to observe the ion state $6a^3$ and $6a^4$ but these would be masked under the $7a^1$ and $7a^16a^1$ peaks respectively. This suggests that the overall intensity of the $1333\,cm^{-1}$ peak may result from a competition between the decay of $7a^1$ and the rise of $6a^3$ in S_1. Thus, from a picosecond time-resolved photoelectron study of the IVR following the excitation of the $7a^1$ level in S_1 *p*FT we have a provisional assignment of a dark state [32].

Continuing with the analysis, we can ask what the minimum number of states is that could account for the time behaviour shown in Figure 10. In order to address this we have used three basis states; the 0 ps spectrum, the 7.5 ps spectrum, and the 1000 ps spectrum. Using these three states we can satisfactorily reproduce the time evolution of the photoelectron spectra, see Figure 11. Thus, according to this analysis, the $7a^1$ bright state need only be coupled to two dark states. This deduction makes an interesting contrast with the implications of earlier work on this mode [4,12] in which congestion in the photoelectron spectra suggested a large number of coupled states, see for example the right panel of Figure 7. This can however be explained if a degree of congestion is there at all times as a result of strong coupling, but does not contribute to the time dependence, as in the scenario illustrated in Figure 6. It is clear that important lessons are contained in these studies regarding how data should be interpreted and how it is easy to be misled by experimental observations. However, the level of detail available in picosecond time-resolved SEVI measurements seems to provide the most promising way forward for unravelling the dynamics of IVR in excited states. Analysis of the data shown in Figure 10 is ongoing, and additional experiments are underway in order to explore the effects of changing bandwidth and temperature, as well as to investigate mode dependence and to compare with similar molecules with slightly modified structure [32].

7.5. *Comparison of pFT and toluene*

Although the various 'health warnings' outlined above need to be taken into account, it is clear that if comparative experiments are performed useful qualitative information can nonetheless be obtained, even from VMI experiments. A case in point concerns an experiment in which we compared *p*-fluorotoluene which had been prepared in its 13^1

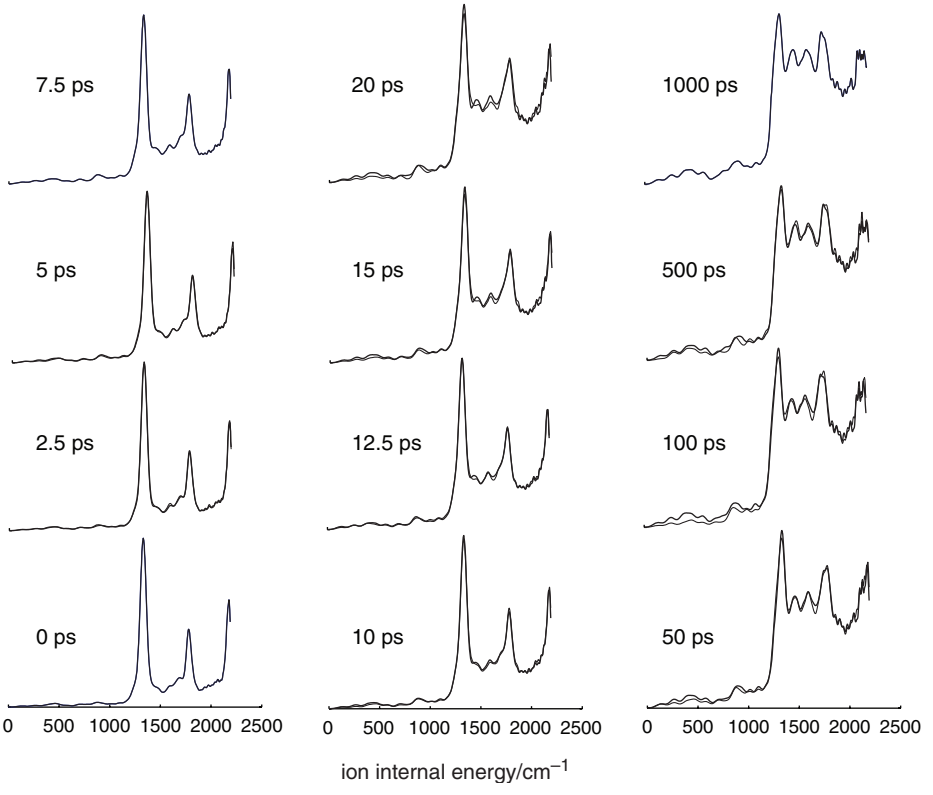

Figure 11. Comparison of the picosecond time-resolved photoelectron spectra shown in Figure 10 with those resulting from a fit to three states [32]. The thick line is the measured photoelectron spectrum and the thin line the fit to the model (see text).

vibrational state in S_1 with toluene which had been prepared in the same vibrational state [32,59]. The validity of the comparison is enhanced by the fact that the vibrational states lie respectively 1194 cm^{-1} and 1193 cm^{-1} above the S_1 origin in the two molecules. In both cases the bright state was prepared with a 1 ps laser pulse, and photoelectron spectra were determined as a function of time delay using VMI following ionization with a probe laser pulse of the same wavelength as the pump. A sample of the results is shown in Figure 12, where it can clearly be seen that the dynamics induced in toluene is far more rapid than that induced in *p*FT. This result has the opposite correlation with the relative torsional barrier heights shown in Table 1 from the one observed for the comparison between *m*FT and *p*FT, however the C–CH_3 stretching mode is adjacent to the centre of flexibility such that the correlation established by Perry and coworkers [51] might be expected to apply in this case. Again, further analysis and data are needed to investigate this further.

8. Conclusion

Whereas eigenstate-resolved studies of IVR in the electronic ground state of a number of molecules have provided robust unambiguous results, the same cannot yet be said

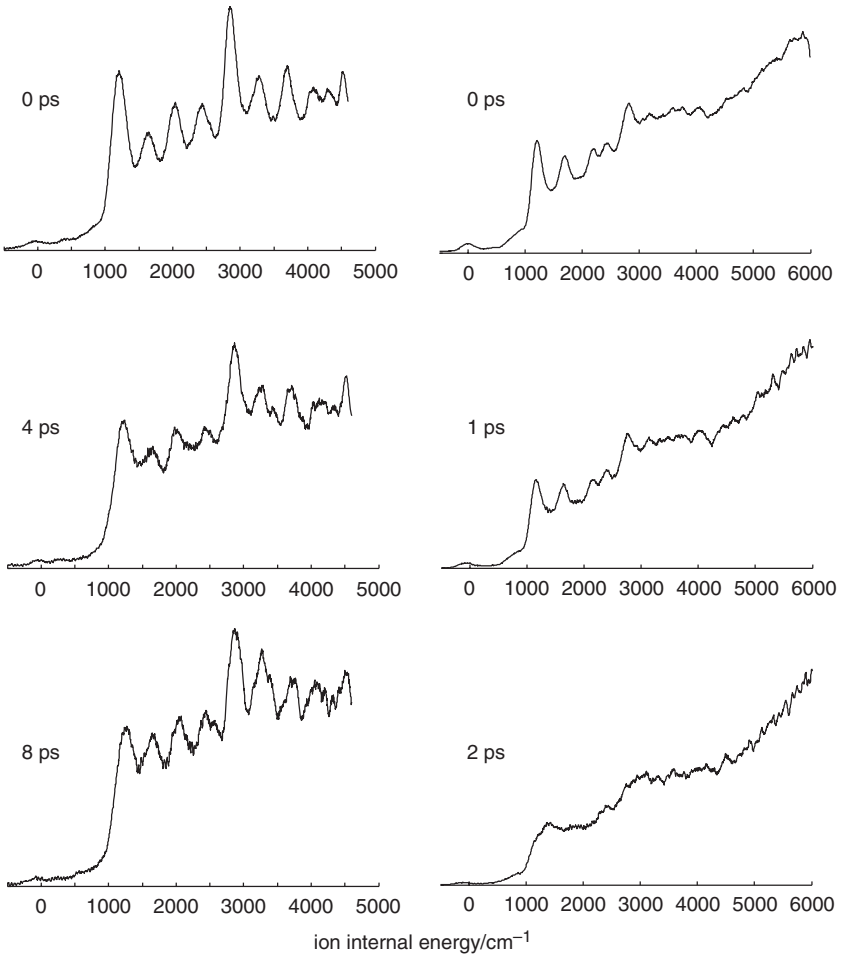

Figure 12. Picosecond time-resolved VMI photoelectron spectra measured following the preparation of the 13^1 ($C–CH_3$ stretching mode) level in *p*-fluorotoluene (left) and toluene (right).

of time-resolved studies of IVR in electronically excited states. Picosecond time-resolved photoelectron spectroscopy provides a method with the capability, in principle, of the identification of dark states populated as a function of time in an IVR process. However, we have shown in this review that great care needs to be taken in order to understand exactly what has been studied, with measurements made under varying experimental conditions. In addition, a full analysis of experimental data is likely to be reliant on good calculations of the Franck–Condon factors that connect the excited state to the ground state of the ion formed.

Acknowledgements

I would like to acknowledge the outstanding contributions of Chris Hammond to this work. All the time-resolved work from our group has been undertaken in the Lasers for Science Facility at the

Rutherford–Appleton Laboratory in Oxfordshire where we have been fortunate to work alongside Drs Mike Towrie, Pavel Matousek and Kate Ronayne. Heroic early experiments were undertaken by Drs Julia Davies, Susan Bellm and Adrian King. Research in this area has been supported by EPSRC grants GR/M83759, GR/R72297 and EP/E046150/1.

Note

1. Note that generally a *rotational* wavepacket will be prepared. However, many experiments will be insensitive to its evolution.

References

[1] A. Stolow, A. E. Bragg, and D. M. Neumark, Chem. Rev. **104**, 1719 (2004).
[2] T. Suzuki, Annu. Rev. Phys. Chem. **57**, 555 (2006).
[3] D. M. Neumark, Annu. Rev. Phys. Chem. **52**, 255 (2001).
[4] C. J. Hammond, V. L. Ayles, D. E. Bergeron, K. L. Reid, and T. G. Wright, J. Chem. Phys. **125**, 124308 (2006).
[5] K. K. Lehmann, G. Scoles, and B. H. Pate, Annu. Rev. Phys. Chem. **45**, 241 (1994).
[6] J. C. Keske and B. H. Pate, Annu. Rev. Phys. Chem. **51**, 323 (2000).
[7] D. R. Borst and D. W. Pratt, J. Chem. Phys. **113**, 3658 (2000).
[8] K. W. Holtzclaw and C. S. Parmenter, J. Chem. Phys. **84**, 1099 (1986).
[9] J. S. Baskin, T. S. Rose, and A. H. Zewail, J. Chem. Phys. **88**, 1458 (1988).
[10] J. M. Smith, C. Lakshminarayan, and J. L. Knee, J. Chem. Phys. **93**, 4475 (1993).
[11] X. B. Song, C. W. Wilkerson, J. Lucia, S. Pauls, and J. P. Reilly, Chem. Phys. Lett. **174**, 377 (1990).
[12] A. K. King, S. M. Bellm, C. J. Hammond, K. L. Reid, M. Towrie, and P. Matousek, Mol. Phys. **103**, 1821 (2005).
[13] R. A. Coveleskie, D. A. Dolson, and C. S. Parmenter, J. Phys. Chem. **89**, 655 (1985).
[14] A. Stolow, Annu. Rev. Phys. Chem. **54**, 89 (2003).
[15] T. Baumert, V. Engel, C. Rottgermann, W. T. Strunz, and G. Gerber, Chem. Phys. Lett. **191**, 639 (1992).
[16] I. Fischer, M. J. J. Vrakking, D. M. Villeneuve, and A. Stolow, Chem. Phys. **207**, 331 (1996).
[17] K. Mueller Dethlefs, M. Sander, and E. W. Schlag, J. Phys. Sci. **39**, 1089 (1984).
[18] F. Merkt, Annu. Rev. Phys. Chem. **48**, 675 (1997).
[19] X. Zhang, J. M. Smith, and J. L. Knee, J. Chem. Phys. **100**, 2429 (1994).
[20] J. M. Smith, C. Lakshminarayan, and J. L. Knee, J. Chem. Phys. **93**, 4475 (1990).
[21] J. M. Smith, X. Zhang, and J. L. Knee, J. Chem. Phys. **99**, 2550 (1993).
[22] A. T. J. B. Eppink and D. H. Parker, Rev. Sci. Instrum. **68**, 3477 (1997).
[23] J. A. Davies, R. E. Continetti, D. W. Chandler, and C. C. Hayden, Phys. Rev. Lett. **84**, 5983 (2000).
[24] B. Baguenard, J. B. Wills, F. Pagliarulo, B. Climen, M. Barbaire, C. Clavier, M. A. Lebeault, and C. Bordas, Rev. Sci. Instrum. **75**, 324 (2004).
[25] S. J. Cavanagh, S. T. Gibson, M. N. Gale, C. J. Dedman, E. H. Roberts, and B. R. Lewis, Phys. Rev. A **76**, 052708 (2007).
[26] T. Suzuki, L. Wang, and H. Kohguchi, J. Chem. Phys. **111**, 4859 (1999).
[27] S. Sorgues, L. Poisson, K. Raffael, L. Krim, B. Soep, and N. Shafizedeh, J. Chem. Phys. **124**, 114302 (2006).
[28] A. Kammrath, G. B. Griffin, J. R. R. Verlet, R. M. Young, and D. M. Neumark, J. Chem. Phys. **126**, 244306 (2007).
[29] R. Mabbs, K. Pichugin, and A. Sanov, J. Chem. Phys. **122**, 174305 (2005).

[30] A. Osterwalder, M. J. Nee, J. Zhou, and D. M. Neumark, J. Chem. Phys. **121**, 6317 (2004).
[31] C. Nicole, I. Sluimer, F. Rosca-Pruna, M. Warntjes, M. Vrakking, C. Bordas, F. Texier, and F. Robicheaux, Phys. Rev. Lett. **85**, 4024 (2000).
[32] C. J. Hammond and K. L. Reid, Phys. Chem. Chem. Phys. DOI: 10.1039/b812254g (2008).
[33] K. L. Reid, Annu. Rev. Phys. Chem. **54**, 397 (2003).
[34] O. Gessner, A. M. D. Lee, J. P. Shaffer, H. Reisler, S. V. Levchenko, A. I. Krylov, J. G. Underwood, H. Shi, A. L. L. East, D. M. Wardlaw, E. T. Chrysostom, C. C. Hayden, and A. Stolow, Science **311**, 219 (2006).
[35] M. Tsubouchi and T. Suzuki, J. Phys. Chem. A **107**, 10897 (2003).
[36] J. A. Davies, C. C. Hayden, unpublished work.
[37] M. Tsubouchi, B. J. Whitaker, L. Wang, H. Kohguchi, and T. Suzuki, Phys. Rev. Lett. **86**, 4500 (2001).
[38] A. E. Bragg, R. Wester, A. V. Davis, A. Kammrath, and D. M. Neumark, Chem. Phys. Lett. **376**, 767 (2003).
[39] P. M. Felker and A. H. Zewail, J. Chem. Phys. **86**, 2460 (1987).
[40] J. G. Underwood and K. L. Reid, J. Chem. Phys. **113**, 1067 (2000).
[41] T. Noguchi, S. Sato, and Y. Fujimara, Chem. Phys. Lett. **155**, 177 (1989).
[42] G. M. Nathanson and G. M. McClelland, J. Chem. Phys. **81**, 629 (1984).
[43] K. L. Reid, T. A. Field, M. Towrie, and P. Matousek, J. Chem. Phys. **111**, 1438 (1999).
[44] S. C. Althorpe and T. Seideman, J. Chem. Phys. **113**, 7901 (2000).
[45] S. M. Bellm, J. A. Davies, P. T. Whiteside, J. Guo, I. Powis, and K. L. Reid, J. Chem. Phys. **122**, 224306 (2005).
[46] G. M. Nathanson and G. M. McClelland, Chem. Phys. Lett. **114**, 441 (1985).
[47] M. Staniforth, A. K. King, I. Powis and K. L. Reid, unpublished work.
[48] C. S. Parmenter and B. M. Stone, J. Chem. Phys. **84**, 4710 (1986).
[49] D. B. Moss, C. S. Parmenter, and G. E. Ewing, J. Chem. Phys. **86**, 51 (1987).
[50] D. B. Moss and C. S. Parmenter, J. Chem. Phys. **98**, 6897 (1993).
[51] D. S. Perry, G. A. Bethardy, and X.-L. Wang, Ber. Bunsenges. Phys. Chem. **99**, 530 (1995).
[52] Z. Q. Zhao, C. S. Parmenter, D. B. Moss, A. J. Bradley, A. E. W. Knight, and K. G. Owens, J. Chem. Phys. **96**, 6362 (1992).
[53] P. J. Timbers, C. S. Parmenter, and D. B. Moss, J. Chem. Phys. **100**, 1028 (1994).
[54] C. J. Hammond, K. L. Reid, and K. L. Ronayne, J. Chem. Phys. **124**, 201102 (2006).
[55] C. G. Hickman, J. R. Gascooke, and W. D. Lawrance, J. Chem. Phys. **104**, 4887 (1996).
[56] S. M. Bellm, P. T. Whiteside, and K. L. Reid, J. Phys. Chem. A **107**, 7373 (2003).
[57] A. K. King, S. M. Bellm, K. L. Reid, M. Towrie and P. Matousek, unpublished work (2005).
[58] V. L. Ayles, C. J. Hammond, D. E. Bergeron, and T. G. Wright, J. Chem. Phys. **126**, 244304 (2006).
[59] P. T. Whiteside, A. K. King, J. A. Davies, K. L. Reid, M. Towrie, and P. Matousek, J. Chem. Phys. **123**, 204317 (2005).
[60] K. Okuyama, N. Mikami, and M. Ito, J. Phys. Chem. **89**, 5617 (1985).